Published in final edited form as:
Neurobiol Aging. 2012 January ; 33(1): 75–82. doi:10.1016/j.neurobiolaging.2010.02.005.

Forebrain-dominant deficit in cerebrovascular reactivity in Alzheimer's Disease

Uma S. Yezhuvath[a], **Jinsoo Uh**[a], **Yamei Cheng**[a], **Kristin Martin-Cook**[b], **Myron Weiner**[b], **Ramon Diaz-Arrastia**[b], **Matthias van Osch**[c], and **Hanzhang Lu**[a,*]

[a] Advanced Imaging Research Center, University of Texas Southwestern Medical Center, Dallas, TX 75390 [b] Alzheimer's Disease Center, University of Texas Southwestern Medical Center, Dallas, TX 75390 [c] Department of Radiology, Leiden University Medical Center, Leiden, The Netherlands

Abstract

Epidemiologic evidence and postmortem studies of cerebral amyloid angiopathy suggest that vascular dysfunction may play an important role in the pathogenesis of Alzheimer's Disease (AD). However, alterations in vascular function under in vivo conditions are poorly understood. In this study, we assessed cerebrovascular-reactivity (CVR) in AD patients and age-matched controls using CO2-inhalation while simultaneously acquiring Blood-Oxygenation-Level-Dependent (BOLD) MR images. Compared to controls, AD patients had widespread reduction in CVR in the rostral brain including prefrontal, anterior cingulate, and insular cortex ($p<0.01$). The deficits could not be explained by cardiovascular risk factors. The spatial distribution of the CVR deficits differed drastically from the regions of cerebral blood flow (CBF) deficits, which were found in temporal and parietal cortices. Individuals with greater CVR deficit tended to have a greater volume of leukoaraiosis as seen on FLAIR MRI ($p=0.004$). Our data suggest that early AD subjects have evidence of significant forebrain vascular contractility deficits. The localization, while differing from CBF findings, appears to be spatially similar to PIB amyloid imaging findings.

Keywords

Alzheimer's Disease; Vascular function; Cerebrovascular reactivity; Magnetic Resonance Imaging; Cerebral blood flow

1. Introduction

Alzheimer's Disease (AD) is a neurodegenerative disease that affects more than four million people in the U.S. alone. Formation and accumulation of extracellular beta-amyloid (Aβ) containing plaques and intra neuronal neurofibrillary tangles consisting of hyperphosphorylated tau are thought to be the central process in AD (Hardy and Selkoe, 2002; Small, 2005). The possibility of a vascular contribution to AD has also received

*Corresponding Author: Hanzhang Lu, Ph.D., Advanced Imaging Research Center, UT Southwestern Medical Center, 5323 Harry Hines Blvd., Dallas, TX 75390, hanzhang.lu@utsouthwestern.edu, Tel: 214-645-2761, Fax: 214-645-2744.

attention (de la Torre, 2004; Iadecola, 2004; Zlokovic, 2005). There is epidemiological evidence that many risk factors for AD relate to vascular disease (e.g. hypertension, hypercholesterolemia, diabetes) (Breteler, 2000; Meyer et al., 2000). Cerebral amyloid angiopathy is commonly observed in postmortem AD studies (Tian et al., 2004). Several studies have further shown that vascular dysfunction can stimulate Aβ accumulation in the brain. Sun et al. (Sun et al., 2006) and Zhang et al. (Zhang et al., 2007) have independently reported that transient hypoxia can cause an increase in the gene expression of β-site of amyloid precursor protein cleaving enzyme (BACE1), the main form of β-secretase, and Aβ production. Therefore, perfusion-induced hypoxia may have a significant impact on the homeostasis of Aβ.

While vascular abnormalities in AD have been studied in postmortem brain tissues (Chow et al., 2007) and in animal models (Meyer et al., 2008), in vivo investigation of vascular dysfunction in AD patients has not been systematically conducted. Measures of resting cerebral blood flow (CBF) (Yoshikawa et al., 2003) or CBF changes during brain activation (as used in functional MRI) (Xu et al., 2007) are not accurate indicators of vascular function, because these measures are highly sensitive to levels of neural activity and are thus not specific to vessel properties. In vitro studies have established that one of the best measures of vessel function is its contractility (Chow et al., 2007). Cerebral vessel reactivity (CVR) can be measured in vivo in humans by the use of CO2 as a vasodilatory stimulus (Rostrup et al., 2000; Kastrup et al., 2001; Yezhuvath et al., 2009), and is the technique employed in our study of brain vasculature in AD.

In the present study, we hypothesized that AD patients would show diminished CVR compared to that of controls and that the degree of CVR impairment would correlate with the degree of leukoaraiosis, a commonly accepted surrogate for microvascular disease.

2. Methods

Participants

Participants were recruited from longitudinal cohorts maintained by the Alzheimer's Disease Center of University of Texas Southwestern Medical Center. The Health Insurance Portability and Accountability Act (HIPAA) compliant protocol was approved by the UT Southwestern Institutional Review Board and written informed consent was obtained from all participants. Inclusion/exclusion criteria for all subjects were: a) No contraindication to MRI scanning (pacemaker, implanted metallic objects, renal/liver disease), b) general good health, with no serious or unstable medical conditions, c) able and willing to provide informed consent (caregivers co-signed consents for AD patients), d) age greater than 50, e) no evidence of stroke in clinical MRI, f) Hachinski (Hachinski et al., 1975) score<4. Additional criteria for the control group were normal cognition and Clinical Dementia Rating (CDR) (Morris, 1993) score=0. For AD group, this included a diagnosis of probable AD based on NINCDS/ADRDA criteria (McKhann et al., 1984) with CDR score = 0.5 or 1. This is a group of mild AD group (MMSE 22.8 ± 4.1) and they were able to follow instructions for the hypercapnia task. Table 1 lists demographic information for the participants.

To assess the effect of vascular factors, we made a scale by summing cardiovascular risk factors (Breteler, 2000; de la Torre, 2004) of the participants (history of cardiovascular disease, stroke or transient ischemic attack, hypertension, hypercholesterolemia, diabetes mellitus and smoking status): each receiving a value of 1 or 0, with a maximum total score of 6. In addition, medications that may affect the vascular risk factors are also listed in Table 1. These include cholesterol-lowering drugs such as statins and anti-hypertensive drugs such

as beta blocker, calcium channel blocker, angiotensin inhibitor, angiotensin converting enzyme inhibitor, and diuretics.

A total of 17 AD patients and 17 elderly controls were recruited. Some participants had incomplete data because they declined the CO2 breathing task or were unable to stay still during the MRI. As a result, the actual sample sizes for CVR, CBF and FLAIR data were 12/13 (AD/control), 15/14 and 15/15, respectively. While this caused the reported vascular parameters to be based on different samples, no differences were seen in the severity across the subgroups as measured by Mini-Mental State Exam (MMSE) (Folstein et al., 1975), CDR and Consortium to Establish a Registry for Alzheimer's Disease (CERAD) (Morris et al., 1989) battery tests.

Experiments

MRI investigations were performed on a 3 Tesla MR system (Philips Medical System, Best, The Netherlands). A body coil was used for radiofrequency (RF) transmission and an 8-channel head coil with parallel imaging capability was used for signal reception. CVR measurement followed protocols established in our previous studies (Yezhuvath et al., 2009). Region-specific CVR was assessed using hypercapnia induced by 5% CO2-breathing (mixed with 21% O2 and 74% N2). Hypercapnia was administered via a Douglas bag with a valve to switch between room air and CO2 air. A mouth piece and nose clip was used to achieve mouth-only breathing. A research assistant was inside the magnet room throughout the experiment to switch the valve and monitor the subject. Physiologic parameters, including end-tidal (Et) CO2, breathing rate, heart rate and arterial oxygenation (sO2), were recorded during experiments (MEDRAD, Pittsburgh, PA; Novametrix Medical Systems, Wallingford, CT). The type of air breathed in was switched every minute similar to a block design fMRI experiment, while Blood-Oxygenation-Level-Dependent (BOLD) MR images were acquired for seven minutes. Other imaging parameters were: FOV=220×220mm^2, matrix size=128×128, 25 axial slices, thickness=6mm, TR/TE/flip angle=3000ms/30ms/90°, single-shot echo-planar-imaging (EPI).

For comparison with CVR, resting CBF was measured using Arterial-Spin-Labeling (ASL) MRI (Garcia D.M., 2005; Wong, 2007; Wu et al., 2007). Scan parameters were: FOV=240×240mm^2, matrix=80×80, 17 axial slices, thickness=7mm, TR/TE=4000ms/14ms, pseudo-continuous labeling with a duration of 1.6s, delay=1.5s, single-shot EPI, 30 pairs of label and control images, duration=240 sec. For assessment of brain volume, a T1-weighted high resolution (1×1×1mm^3) anatomical image using magnetization-prepared rapid acquisition of gradient echo (MPRAGE) sequence (Brant-Zawadzki et al., 1992) was acquired. We also acquired Fluid-Attenuated Inversion Recovery (FLAIR) images (Essig et al., 1998) (TR/TI/TE=11000ms/2800ms/125ms, FOV=230×230mm^2, resolution=0.45×0.45mm^2, 24 slices, thickness=5mm, gap=1mm) for quantifying volume of leukoaraiosis. The total MRI examination was approximately 30 minutes.

Neuropsychological test results including MMSE, CERAD Battery, CDR, and Boston Naming Test (Kaplan E.F., 1978) were available for comparison with MRI data.

Data Processing

CVR data was processed using a general linear model (SPM, University College London, UK) similar to a typical fMRI scan, except that the regressor was the EtCO2 time-course rather than the "fMRI paradigm". In-house MATLAB scripts were used to obtain EtCO2 time-courses that were synchronized with MRI acquisitions. Since the hypercapnia-induced vasodilatation is mediated through CO2 level changes, EtCO2 time-course provides an input function to the vascular system. The BOLD time-course is the output signal and, by

comparing the input and output signals, the vascular system property was determined (Yezhuvath et al., 2009). Absolute CVR is in units of %BOLD signal change per mmHg of Et-CO2 change (%BOLD/mmHg CO2). In addition, relative CVR map was calculated by normalizing the absolute CVR map against the CVR of a reference tissue, which was chosen to be cerebellum (Soonawala et al., 2002) because it is reasonably well established that cerebellum is minimally affected in AD. The conversion of absolute CVR to relative CVR was useful in removing global intersubject variability and facilitates the detection of regional deficits (Yezhuvath et al., 2009).

ASL MR images were used to calculate CBF by subtraction of the control and label image sets following procedures established previously (Lia et al., 2000). The 30 repeated scans were averaged to improve SNR. Relative CBF maps were obtained for each subject.

The CVR and CBF maps were further processed with Statistical Parametric Mapping (SPM, University College London, UK) and Hierarchical Attribute Matching Mechanism for Elastic Registration (HAMMER, University of Pennsylvania, PA) software packages. The maps were normalized to the Montreal Neurological Institute (MNI) template space using the high-resolution T1w image as an intermediate and were smoothed using a filter with full-width-half-maximum 12mm. We used a HAMMER algorithm for the spatial normalization process because it was shown to be capable of correcting brain atrophy effects (Shen and Davatzikos, 2002). This was important to make sure the comparison truly reflected vascular parameters rather than being affected by brain volume reduction, especially for AD patients who often have brain atrophy (Buckner et al., 2005).

For voxel-by-voxel analysis of CVR and CBF maps, we conducted a multiple regression analysis with subject group, age and vascular risk factor as the regressors. Student t tests were conducted to identify significant clusters using criteria established in literature (Xu et al., 2007). We also performed a region-of-interest (ROI) analysis on the normalized images. ROI corresponding to different brain lobes was automatically determined using the pre-parcellated MNI brain template (Tzourio-Mazoyer et al., 2002). Six ROIs were investigated: occipital lobe, temporal lobe, frontal lobe, parietal lobe, insular cortex and sub-cortical gray matter. The vessel reactivity within the ROI was averaged. To account for gray/white matter reactivity differences and correct for residual atrophy at the intravoxel level, the ROI value was corrected for gray matter volume following procedures used previously (Johnson et al., 2005). A multi-comparison-corrected p value of 0.05 or less is considered significant.

The leukoaraiosis regions were identified with a semi-automatic method (Marquez de la Plata et al., 2007; Uh et al., 2009). Briefly, FLAIR images were skull-stripped and voxels with signal intensity greater than 2 standard deviations above average were delineated as a preliminary mask. This preliminary mask was manually edited to remove spurious voxels due to fat signal, motion effect, edge effect, or coil sensitivity inhomogeneity. The total volume within the final mask was quantified for each subject. The procedure was highly reliable (r^2=0.99) (data not shown). For correlation analysis, Pearson correlation coefficients were calculated. We also calculated Spearman rank correlation to assess the possible influence of outliers. A p value of 0.05 or less is considered statistically significant.

3. Results

AD subjects and controls performed the CO2 task comfortably and no adverse effect was observed. Table 2 shows the vital sign values for each group. As expected, Et-CO2 increased during CO2 inhalation. Breathing rate, heart rate and arterial oxygen saturation did not differ significantly between normocapnic and hypercapnic conditions. No group differences in vital signs were observed. Figure 1A shows the relative CVR maps for AD

(left) and control (right) groups. Reduced CVR is evident in rostral brain regions of AD subjects. Quantitative analysis showed that significant CVR deficits were present in prefrontal, anterior cingulate, and insular cortices in AD patients compared to control subjects (Fig. 1B). ROI analysis revealed similar results, identifying frontal lobe (corrected p=0.047) and insula (corrected p=0.037) having reduced CVR. On the other hand, CBF deficit patterns (see CBF maps in Fig. 2A and voxel-based results in Fig. 2B) included predominantly posterior regions. These CBF deficits in temporal and parietal lobes agree with previous CBF studies in AD using SPECT, PET and MRI (Alsop et al., 2000;Johannsen et al., 2000;Yoshikawa et al., 2003;Johnson et al., 2005).

The AD group had slightly higher vascular risk factor scores than controls (Table 1), although the difference did not reach statistical significance (p=0.17). When we defined the statistical contrast in the voxel-based analysis to be vascular risk factors, no significant clusters were identified for either a positive effect or a negative effect and for either CVR or CBF data. Consistent with this finding, when we omitted the risk factors from the multi-regression analysis, the AD/Control group difference was not affected.

To test the hypothesis that CVR may be related to high risk for vascular damage, we used relative CVR of 0.1 as a threshold and identified all voxels with a CVR value equal to or less than the threshold. We presumed that these voxels reflect brain regions with minimal vascular reserve and diminished ability to dilate with CO2 stimulation. We quantified the total volume of these “high-risk” regions and calculated its correlation with the volume of leukoaraiosis (Fig. 3A). A strong positive correlation was found between these measures (Pearson r^2=0.67, p=0.004, Spearman rank p=0.014, N=10) (Fig. 3B). We also tested relative CVR thresholds of 0, 0.05 and 0.15, and found similar results (Table 3). On the other hand, when applying similar criteria to the CBF measures, the correlation between leukoaraiosis volume and CBF deficit volume was much weaker (Pearson r^2=0.32, p=0.043, Spearman rank p=0.189, N=13) (Fig. 3C, Table 3).

Given the pronounced CVR deficits in AD patients, we hypothesized that patients with lower CVR would have more severe cognitive impairment. We conducted correlation analysis between the CVR value in frontal lobe and insula (the primary CVR deficit regions) and each of the cognitive score. We did not find a relationship between CVR and measures of global cognitive function (MMSE, CERAD Battery, CDR), but found a significant correlation between CVR and Boston Naming Test score (Pearson r^2=0.43, p=0.021, Spearman Rank p=0.002, N=12).

4. Discussion

This study employed an in vivo imaging technique to assess cerebrovascular endothelial and smooth muscle function independent of neuronal metabolism or activity. To our knowledge, this is the first in vivo study of regional CVR in AD patients. Using a novel CO2-inhalation MRI technique, we were able to non-invasively measure CVR. We found widespread CVR deficits in the rostral brain of persons with early AD, highly suggestive of vascular dysfunction in AD uninfluenced by the number of cardiovascular risk factors such as hypertension, hypercholesterolemia and diabetes mellitus.

Our findings of vascular dysfunction in the frontal regions coincide with in vivo amyloid mapping results using Pittsburgh Compound B (PiB) (Klunk et al., 2004; Buckner et al., 2005; Buckner et al., 2009), and suggest that vascular damage and amyloid deposition (in particular in the form of vascular amyloid) may have a potential link. This notion is consistent with postmortem studies showing that Aβ can have a detrimental effect on brain vasculature via cerebral amyloid angiopathy (Beckmann et al., 2003; Tian et al., 2004).

Conversely, a disturbed vascular system can cause over-expression of APP and β-secretase in animal models of AD (Sun et al., 2006; Zhang et al., 2007), which may result in Aβ formation. A multi-modal study combining PET amyloid and MRI vascular reactivity measures in the same patient group would be useful in further elucidating the relationship between Aβ and vascular function in AD.

It is well known that patients with AD have reduced CBF in parietal and temporal regions (Alsop et al., 2000; Yoshikawa et al., 2003; Johnson et al., 2005). However, the interpretation of these findings is not straightforward. There are at least two possible causes for the CBF reduction: 1) vascular dysfunction (similar to ischemia) or 2) lower metabolism of the tissue (i.e. lower demand causing lower supply). Based on current evidence, it appears that the reduced CBF observed in AD patients is mainly due to the latter mechanism, with minimal implication of vascular health. This is supported by our findings of drastically different spatial locations of CVR and CBF deficits. Furthermore, when we averaged the CVR values in CBF deficit regions (i.e. colored areas in Fig. 2B), we found that the CVR values were 0.25±0.10 %BOLD/mmHg and 0.22±0.05 %BOLD/mmHg for AD and controls, respectively. There was not even a trend of CVR reduction in the CBF deficit regions ($p=0.269$). If anything, CVR in temporoparietal areas was slightly higher in AD than in controls. By contrast, the CBF deficit pattern is very similar to deficits of glucose metabolism in AD patients as demonstrated with fluorodeoxyglucose (FDG) PET (Small et al., 2000; Reiman et al., 2005). These findings suggest that previous CBF studies mainly reflect tissue metabolic dysfunction, and for assessment of vascular health a more direct index such as vascular reactivity needs to be employed (Terborg et al., 2000; Hund-Georgiadis et al., 2003; Schroeter et al., 2007; Schroeter et al., 2009).

Our parametric comparison of CVR and CBF accounted for brain volume differences between the subject groups, and thus contains minimal partial volume effect. This was achieved by first conducting an elastic brain registration and then comparing CVR and CBF per unit volume of parenchyma. A by-product of the elastic registration is the parenchyma density map which confirmed the well known brain atrophy in AD patients (Buckner et al., 2005).

The findings from the present study are limited in a number of respects. Our sample size was modest. While the number of subjects in this study was sufficient to identify CVR differences in both voxel-based and ROI-based analyses, it would be useful to confirm these findings with a larger study. In particular, not all participants yielded complete data sets. Thus the comparison of CVR, CBF and FLAIR results was obtained from slightly different samples. In addition, a small sample size may result in potential sampling bias due to heterogeneities in subject characteristics in terms of genetic and environmental factors as well as effects of medications. Our failure to find a correlation between our summation of cardiovascular risk factors and brain vascular parameters as has been reported in many other studies (Jennings et al., 2008; Iadecola et al., 2009) may be due to the insensitivity of our measure, which did not include severity of hypertension or diabetes. Additionally, the effect of cardiovascular medications may be another confounding factor in our assessment of vascular risks.

5. Conclusion

Significant deficits in vessel reactivity are present in early AD patients. These deficits are most pronounced in rostral brain regions including prefrontal, anterior cingulate and insular cortices, and coincide with PIB rather than CBF findings, raising the possibility of an interaction between Aβ and vascular reactivity.

Acknowledgments

The authors are grateful to Drs. Charles White, Karen Rodrigue and Kristen Kennedy for helpful discussions. This work was supported by Alzheimer Association NIRG 05-14056, National Institutes of Health R01 MH084021, R21 AG034318, R01 AG033106, P30 AG12300, and American Heart Association.

References

Alsop DC, Detre JA, Grossman M. Assessment of cerebral blood flow in Alzheimer's disease by spin-labeled magnetic resonance imaging. Ann Neurol. 2000; 47:93–100. [PubMed: 10632106]

Beckmann N, Schuler A, Mueggler T, Meyer EP, Wiederhold KH, Staufenbiel M, Krucker T. Age-dependent cerebrovascular abnormalities and blood flow disturbances in APP23 mice modeling Alzheimer's disease. J Neurosci. 2003; 23:8453–8459. [PubMed: 13679413]

Brant-Zawadzki M, Gillan GD, Nitz WR. MP RAGE: a three-dimensional, T1-weighted, gradient-echo sequence--initial experience in the brain. Radiology. 1992; 182:769–775. [PubMed: 1535892]

Breteler MM. Vascular risk factors for Alzheimer's disease: an epidemiologic perspective. Neurobiol Aging. 2000; 21:153–160. [PubMed: 10867200]

Buckner RL, Sepulcre J, Talukdar T, Krienen FM, Liu H, Hedden T, Andrews-Hanna JR, Sperling RA, Johnson KA. Cortical hubs revealed by intrinsic functional connectivity: mapping, assessment of stability, and relation to Alzheimer's disease. J Neurosci. 2009; 29:1860–1873. [PubMed: 19211893]

Buckner RL, Snyder AZ, Shannon BJ, LaRossa G, Sachs R, Fotenos AF, Sheline YI, Klunk WE, Mathis CA, Morris JC, Mintun MA. Molecular, structural, and functional characterization of Alzheimer's disease: evidence for a relationship between default activity, amyloid, and memory. J Neurosci. 2005; 25:7709–7717. [PubMed: 16120771]

Chow N, Bell RD, Deane R, Streb JW, Chen J, Brooks A, Van Nostrand W, Miano JM, Zlokovic BV. Serum response factor and myocardin mediate arterial hypercontractility and cerebral blood flow dysregulation in Alzheimer's phenotype. Proc Natl Acad Sci U S A. 2007; 104:823–828. [PubMed: 17215356]

de la Torre JC. Is Alzheimer's disease a neurodegenerative or a vascular disorder? Data, dogma, and dialectics. Lancet Neurol. 2004; 3:184–190. [PubMed: 14980533]

Essig M, Hawighorst H, Schoenberg SO, Engenhart-Cabillic R, Fuss M, Debus J, Zuna I, Knopp MV, van Kaick G. Fast fluid-attenuated inversion-recovery (FLAIR) MRI in the assessment of intraaxial brain tumors. J Magn Reson Imaging. 1998; 8:789–798. [PubMed: 9702879]

Folstein MF, Folstein SE, McHugh PR. "Mini-mental state". A practical method for grading the cognitive state of patients for the clinician. J Psychiatr Res. 1975; 12:189–198. [PubMed: 1202204]

Garcia, DMdBC.; Alsop, D. Pseudo-continuous Flow Driven Adiabatic Inversion for Arterial Spin Labeling. Intl Soc Mag Reson Med. 2005

Hachinski VC, Iliff LD, Zilhka E, Du Boulay GH, McAllister VL, Marshall J, Russell RW, Symon L. Cerebral blood flow in dementia. Arch Neurol. 1975; 32:632–637. [PubMed: 1164215]

Hardy J, Selkoe DJ. The amyloid hypothesis of Alzheimer's disease: progress and problems on the road to therapeutics. Science. 2002; 297:353–356. [PubMed: 12130773]

Hund-Georgiadis M, Zysset S, Naganawa S, Norris DG, Von Cramon DY. Determination of cerebrovascular reactivity by means of FMRI signal changes in cerebral microangiopathy: a correlation with morphological abnormalities. Cerebrovasc Dis. 2003; 16:158–165. [PubMed: 12792174]

Iadecola C. Neurovascular regulation in the normal brain and in Alzheimer's disease. Nat Rev Neurosci. 2004; 5:347–360. [PubMed: 15100718]

Iadecola C, Park L, Capone C. Threats to the mind: aging, amyloid, and hypertension. Stroke. 2009; 40:S40–44. [PubMed: 19064785]

Jennings JR, Muldoon MF, Whyte EM, Scanlon J, Price J, Meltzer CC. Brain imaging findings predict blood pressure response to pharmacological treatment. Hypertension. 2008; 52:1113–1119. [PubMed: 18981325]

Johannsen P, Jakobsen J, Gjedde A. Statistical maps of cerebral blood flow deficits in Alzheimer's disease. Eur J Neurol. 2000; 7:385–392. [PubMed: 10971597]

Johnson NA, Jahng GH, Weiner MW, Miller BL, Chui HC, Jagust WJ, Gorno-Tempini ML, Schuff N. Pattern of cerebral hypoperfusion in Alzheimer disease and mild cognitive impairment measured with arterial spin-labeling MR imaging: initial experience. Radiology. 2005; 234:851–859. [PubMed: 15734937]

Kaplan, EFGH.; Weintraub, S. The boston naming test. Philadelphia: Lea & Febiger; 1978.

Kastrup A, Kruger G, Neumann-Haefelin T, Moseley ME. Assessment of cerebrovascular reactivity with functional magnetic resonance imaging: comparison of CO(2) and breath holding. Magn Reson Imaging. 2001; 19:13–20. [PubMed: 11295341]

Klunk WE, Engler H, Nordberg A, Wang Y, Blomqvist G, Holt DP, Bergstrom M, Savitcheva I, Huang GF, Estrada S, Ausen B, Debnath ML, Barletta J, Price JC, Sandell J, Lopresti BJ, Wall A, Koivisto P, Antoni G, Mathis CA, Langstrom B. Imaging brain amyloid in Alzheimer's disease with Pittsburgh Compound-B. Ann Neurol. 2004; 55:306–319. [PubMed: 14991808]

Lia TQ, Guang Chen Z, Ostergaard L, Hindmarsh T, Moseley ME. Quantification of cerebral blood flow by bolus tracking and artery spin tagging methods. Magn Reson Imaging. 2000; 18:503–512. [PubMed: 10913711]

Marquez de la Plata C, Ardelean A, Koovakkattu D, Srinivasan P, Miller A, Phuong V, Harper C, Moore C, Whittemore A, Madden C, Diaz-Arrastia R, Devous M Sr. Magnetic resonance imaging of diffuse axonal injury: quantitative assessment of white matter lesion volume. J Neurotrauma. 2007; 24:591–598. [PubMed: 17439343]

McKhann G, Drachman D, Folstein M, Katzman R, Price D, Stadlan EM. Clinical diagnosis of Alzheimer's disease: report of the NINCDS-ADRDA Work Group under the auspices of Department of Health and Human Services Task Force on Alzheimer's Disease. Neurology. 1984; 34:939–944. [PubMed: 6610841]

Meyer EP, Ulmann-Schuler A, Staufenbiel M, Krucker T. Altered morphology and 3D architecture of brain vasculature in a mouse model for Alzheimer's disease. Proc Natl Acad Sci U S A. 2008; 105:3587–3592. [PubMed: 18305170]

Meyer JS, Rauch GM, Rauch RA, Haque A, Crawford K. Cardiovascular and other risk factors for Alzheimer's disease and vascular dementia. Ann N Y Acad Sci. 2000; 903:411–423. [PubMed: 10818532]

Morris JC. The Clinical Dementia Rating (CDR): current version and scoring rules. Neurology. 1993; 43:2412–2414. [PubMed: 8232972]

Morris JC, Heyman A, Mohs RC, Hughes JP, van Belle G, Fillenbaum G, Mellits ED, Clark C. The Consortium to Establish a Registry for Alzheimer's Disease (CERAD). Part I. Clinical and neuropsychological assessment of Alzheimer's disease. Neurology. 1989; 39:1159–1165. [PubMed: 2771064]

Reiman EM, Chen K, Alexander GE, Caselli RJ, Bandy D, Osborne D, Saunders AM, Hardy J. Correlations between apolipoprotein E epsilon4 gene dose and brain-imaging measurements of regional hypometabolism. Proc Natl Acad Sci U S A. 2005; 102:8299–8302. [PubMed: 15932949]

Rostrup E, Law I, Blinkenberg M, Larsson HB, Born AP, Holm S, Paulson OB. Regional differences in the CBF and BOLD responses to hypercapnia: a combined PET and fMRI study. Neuroimage. 2000; 11:87–97. [PubMed: 10679182]

Schroeter ML, Stein T, Maslowski N, Neumann J. Neural correlates of Alzheimer's disease and mild cognitive impairment: a systematic and quantitative meta-analysis involving 1351 patients. Neuroimage. 2009; 47:1196–1206. [PubMed: 19463961]

Schroeter ML, Cutini S, Wahl MM, Scheid R, Yves von Cramon D. Neurovascular coupling is impaired in cerebral microangiopathy--An event-related Stroop study. Neuroimage. 2007; 34:26–34. [PubMed: 17070070]

Shen D, Davatzikos C. HAMMER: hierarchical attribute matching mechanism for elastic registration. IEEE Trans Med Imaging. 2002; 21:1421–1439. [PubMed: 12575879]

Small GW, Ercoli LM, Silverman DH, Huang SC, Komo S, Bookheimer SY, Lavretsky H, Miller K, Siddarth P, Rasgon NL, Mazziotta JC, Saxena S, Wu HM, Mega MS, Cummings JL, Saunders AM, Pericak-Vance MA, Roses AD, Barrio JR, Phelps ME. Cerebral metabolic and cognitive

decline in persons at genetic risk for Alzheimer's disease. Proc Natl Acad Sci U S A. 2000; 97:6037–6042. [PubMed: 10811879]

Small SA. Alzheimer disease, in living color. Nat Neurosci. 2005; 8:404–405. [PubMed: 15795742]

Soonawala D, Amin T, Ebmeier KP, Steele JD, Dougall NJ, Best J, Migneco O, Nobili F, Scheidhauer K. Statistical parametric mapping of (99m)Tc-HMPAO-SPECT images for the diagnosis of Alzheimer's disease: normalizing to cerebellar tracer uptake. Neuroimage. 2002; 17:1193–1202. [PubMed: 12414259]

Sun X, He G, Qing H, Zhou W, Dobie F, Cai F, Staufenbiel M, Huang LE, Song W. Hypoxia facilitates Alzheimer's disease pathogenesis by up-regulating BACE1 gene expression. Proc Natl Acad Sci U S A. 2006; 103:18727–18732. [PubMed: 17121991]

Terborg C, Gora F, Weiller C, Rother J. Reduced vasomotor reactivity in cerebral microangiopathy: a study with near-infrared spectroscopy and transcranial Doppler sonography. Stroke. 2000; 31:924–929. [PubMed: 10754000]

Tian J, Shi J, Bailey K, Mann DM. Relationships between arteriosclerosis, cerebral amyloid angiopathy and myelin loss from cerebral cortical white matter in Alzheimer's disease. Neuropathol Appl Neurobiol. 2004; 30:46–56. [PubMed: 14720176]

Tzourio-Mazoyer N, Landeau B, Papathanassiou D, Crivello F, Etard O, Delcroix N, Mazoyer B, Joliot M. Automated anatomical labeling of activations in SPM using a macroscopic anatomical parcellation of the MNI MRI single-subject brain. Neuroimage. 2002; 15:273–289. [PubMed: 11771995]

Uh J, Lewis-Amezcua K, Martin-Cook K, Cheng Y, Weiner M, Diaz-Arrastia R, Devous M Sr, Shen D, Lu H. Cerebral blood volume in Alzheimer's disease and correlation with tissue structural integrity. Neurobiol Aging. 2009

Wong EC. Vessel-encoded arterial spin-labeling using pseudocontinuous tagging. Magn Reson Med. 2007; 58:1086–1091. [PubMed: 17969084]

Wu WC, Fernandez-Seara M, Detre JA, Wehrli FW, Wang J. A theoretical and experimental investigation of the tagging efficiency of pseudocontinuous arterial spin labeling. Magn Reson Med. 2007; 58:1020–1027. [PubMed: 17969096]

Xu G, Antuono PG, Jones J, Xu Y, Wu G, Ward D, Li SJ. Perfusion fMRI detects deficits in regional CBF during memory-encoding tasks in MCI subjects. Neurology. 2007; 69:1650–1656. [PubMed: 17954780]

Yezhuvath US, Lewis-Amezcua K, Varghese R, Xiao G, Lu H. On the assessment of cerebrovascular reactivity using hypercapnia BOLD MRI. NMR Biomed. 2009

Yoshikawa T, Murase K, Oku N, Imaizumi M, Takasawa M, Rishu P, Kimura Y, Ikejiri Y, Kitagawa K, Hori M, Hatazawa J. Heterogeneity of cerebral blood flow in Alzheimer disease and vascular dementia. AJNR Am J Neuroradiol. 2003; 24:1341–1347. [PubMed: 12917125]

Zhang X, Zhou K, Wang R, Cui J, Lipton SA, Liao FF, Xu H, Zhang YW. Hypoxia-inducible factor 1alpha (HIF-1alpha)-mediated hypoxia increases BACE1 expression and beta-amyloid generation. J Biol Chem. 2007; 282:10873–10880. [PubMed: 17303576]

Zlokovic BV. Neurovascular mechanisms of Alzheimer's neurodegeneration. Trends Neurosci. 2005; 28:202–208. [PubMed: 15808355]

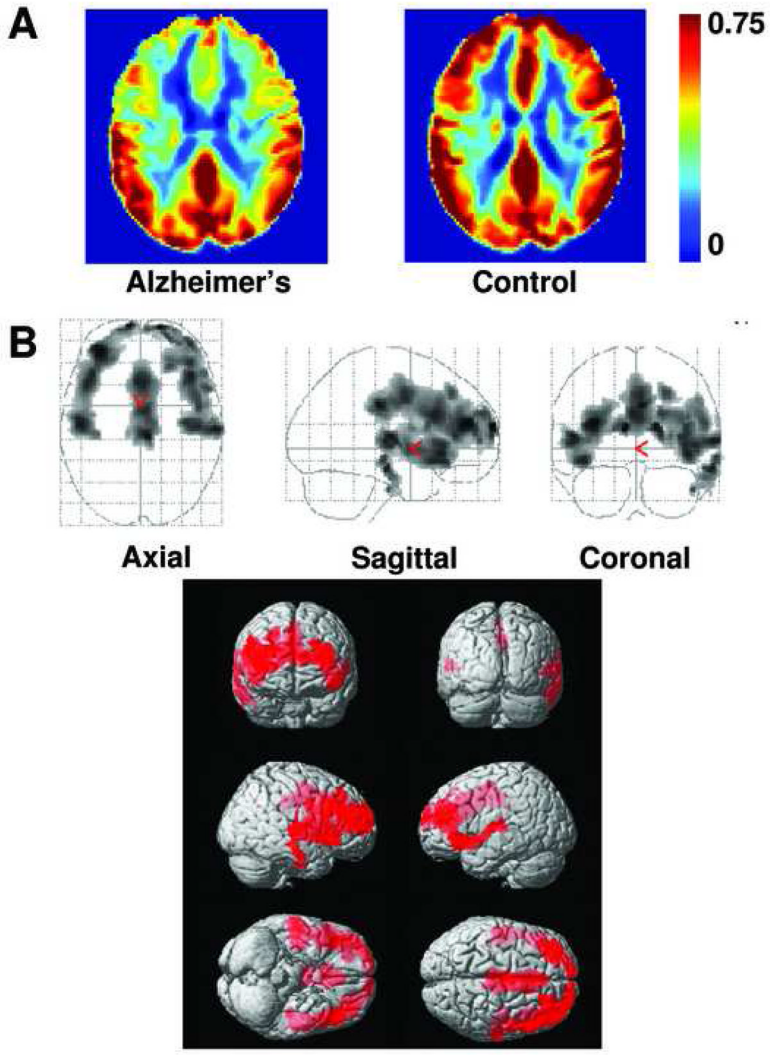

Fig. 1.

Comparison of relative CVR maps in AD and controls. (A) Averaged CVR maps in the patient (left panel, N=12) and control (right panel, N=13) groups. Warmer color indicates a higher CVR value. Color bar shows the range of 0 to 0.75 times the cerebellar CVR. (B) Voxel-based maps of age-corrected and vascular risk factor-corrected CVR differences between AD and controls. The top panel shows the glass brain overlay and the bottom panel shows the rendering on the MNI brain template. Colored voxels indicate brain regions with low CVR. These include prefrontal cortex, anterior cingulate cortex and insular cortex.

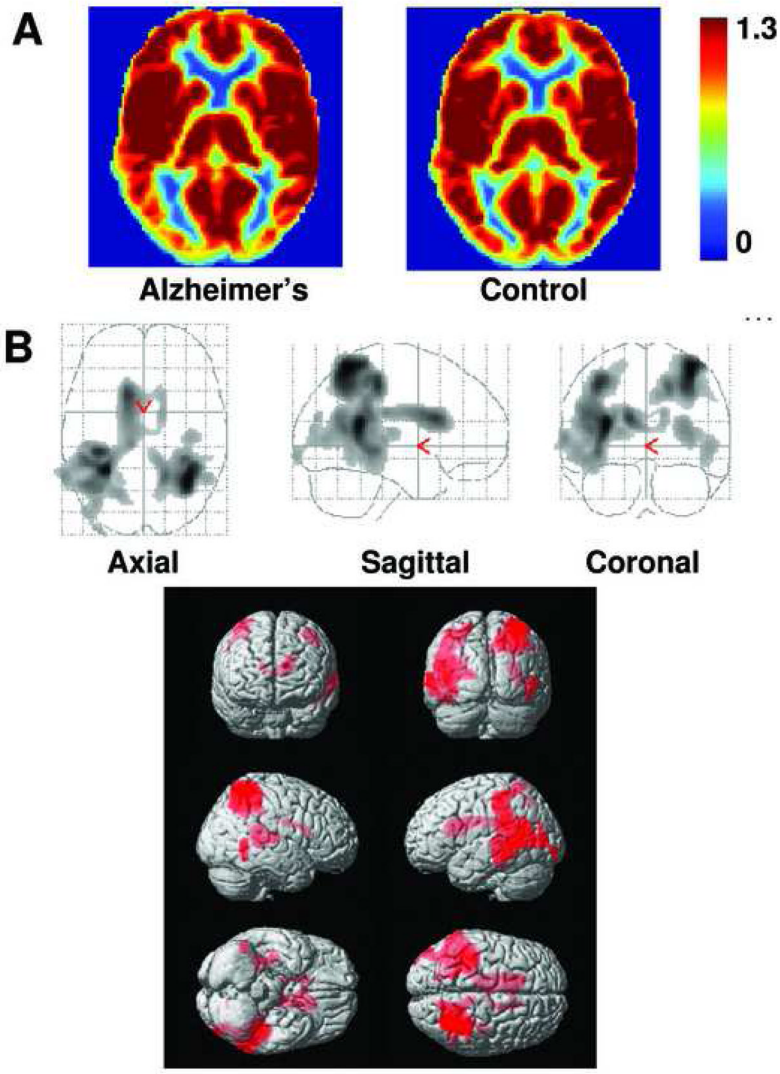

Fig. 2.

Comparison of relative CBF maps in AD and controls. (A) Averaged CBF maps in the patient (left panel, N=15) and control (right panel, N=14) groups. Warmer color indicates a higher CBF value. Color bar shows the range of 0 to 1.3 times the whole-brain CBF. (B) Voxel-based maps of age-corrected and vascular risk factor-corrected CBF differences between AD and controls. The top panel shows the glass brain overlay and the bottom panel shows the rendering on the MNI brain template. Colored voxels indicate brain regions with CBF deficits. The deficits are most pronounced in temporoparietal cortex.

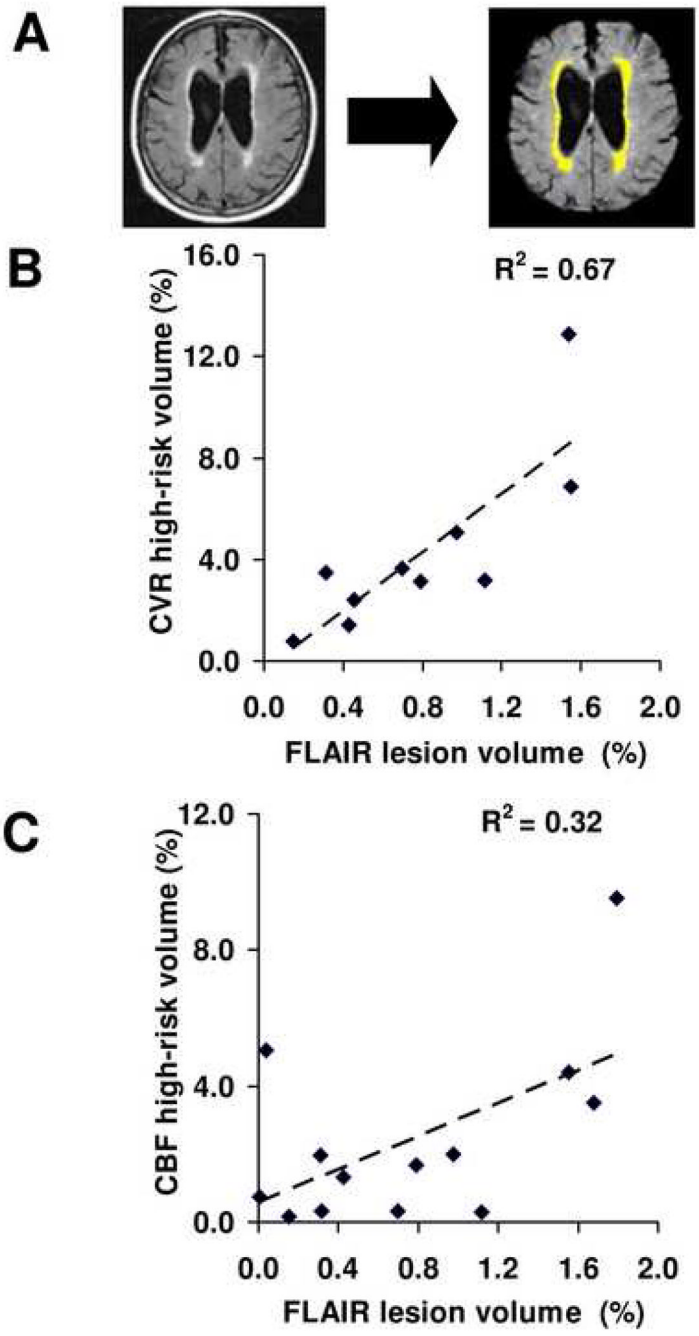

Fig. 3.

Relationship between FLAIR lesion volume and CVR/CBF deficit volumes in AD patients. (A) Tissue lesions were delineated based on the FLAIR MR images using a semi-automatic method reported previously. (B) Scatter plot between FLAIR lesion volume and CVR high-risk volume across patients. Each dot represents data from one patient. The volumes are written in term of fractions of the whole brain white matter volume. A strong positive correlation (p=0.004) is seen between these two parameters. (C) Scatter plot between FLAIR lesion volume and CBF high-risk volume across patients. A weak correlation is observed (p=0.043).

Table 1

Characteristics of AD subjects and controls.

Characteristic	AD Group	Control Group
Number of subjects	17	17
Mean age ± std	70.5 ± 8.3	68.7 ± 8.4
Gender		
Male	13	7
Female	4	10
Education (years) ± std	15.9 ± 2.5	16.5 ± 2.5
MMSE[a] score ± std	22.8 ± 4.1	29.6 ± 0.7
ApoE4 carrier	10/17	6/17
Cardiovascular risk factors[b] ± std	2.2 ± 0.9	1.6 ± 1.3
Cholesterol lowering medications	14/17	8/17
Antihypertensive medications[c]	14/17	7/17

[a] Mini-mental State Exam

[b] See text for definition of the risk factor score.

[c] Includes beta blocker, calcium channel blocker, angiotensin inhibitor, angiotensin converting enzyme inhibitor, and diuretics.

Table 2

Vital signs during room-air breathing and 5% CO2 inhalation (mean ± standard deviation).

	End tidal CO2 (mmHg)		Breathing rate (breaths/min)		Heart Rate (beats/min)		Arterial oxygen saturation (%)	
Subject Category	**Room-Air**	**CO2**	**Room-Air**	**CO2**	**Room-Air**	**CO2**	**Room-Air**	**CO2**
AD (N=12)	33.9±3.5	45.8±1.6	13.0±3.6	13.5±3.9	66.9±10.3	66.8±10.2	97.9±0.8	98.0±0.8
Control (N=13)	33.7±5.3	45.9±3.9	11.7±3.5	11.8±3.9	60.7±8.1	60.3±8.3	97.3±0.9	97.4±0.9

Table 3

Pearson Correlation (r^2 value) between leukoaraiosis volume and high-risk tissue volume using different vascular parameters and thresholds.

Threshold	0	0.05	0.1	0.15
FLAIR vs. CVR	0.51	0.63	0.67	0.52
FLAIR vs. CBF	0.29	0.31	0.32	0.32